Effectiveness of brush parameters in a robotically removal of glovebox debris *

Bechir Tabia[1][0000−0001−8666−1990], Ioannis Zoulias[1][0000−0002−6107−8149], and Guy Burroughes[1][0000−0001−8431−4637]

United Kingdom Atomic Energy Authority, Culham Science Centre, United Kingdom

Abstract. Surface decontamination is essential in Nuclear Gloveboxes, moving this process from manual to robotic would reduce risk to operators. Towards the development of a robotically and autonomous sweeping system, brushing debris removal effectiveness is evaluated using visual inspection with three types of dry simulacrum debris: flour, sand, and metallic swarf. Debris removal effectiveness evaluate the cleanliness rate of a surface and involves environmental parameters such as debris particle size and friction; and also operational parameters such as brush angle of attack, brush penetration, and the number of sweeps. This experiment tested three brush angles of attack and brush penetration using a robotic manipulator arm and repeating a slow and steady rectangle sweeping pattern in a nuclear glovebox. We found that the brush angle of attack has a higher impact than the brush penetration. Also, flour is fast to remove from a surface and necessitates 80 degrees angle of attack. For sand particles, the best configuration is given by a 70-degrees angle of attack to create a contact surface. Regarding debris like metallic swarf, debris particles to bristles bond must be limited, and the required angle of attack is 90 degrees. These results allowed us to determine that autonomous robotic systems must adapt brushing operative parameters to debris type for an effective debris removal process.

Keywords: Nuclear Dismantling · Surface Decontamination · Robotic sweeping · Debris Collection · Brushing Effectiveness.

1 Introduction

In nuclear gloveboxes, surface decontamination are essential in the dismantling process. They ensure the safety of workers and the maintenance of the glovebox by limiting the accumulation on surfaces of hazardous contaminants such as radioactive or toxic material [10] [2]. Currently, human operators are put at considerable risk to perform the cleaning task using tools such as vacuum cleaners, brushes and wet wipes. The choice of technique follows the quantity of debris to collect and the complexity of the cleaning operation. In nuclear gloveboxes, dismantling activities are not safe despite the contained area, and accidents involving operator radioactive contamination by cutting have occurred

* Supported by the United Kingdom Atomic Energy Authority.

in the past [13]. Thus, robotics are being investigated for dismantling activities in nuclear gloveboxes, to limit these accidents and increase workers' safety. Consequently, the RAIN hub develops a robot-assisted nuclear glovebox that allows autonomous, semi-autonomous and remote handling operations [18]. The new robot-assisted nuclear glovebox consists of a pair of robotic manipulator arms and sensors replacing/augment the human operator in gloveboxes. In the long run, the objective is to make the robot perform autonomous dismantling operations such as object size reduction (cutting, drilling), object disassembling, and cleaning (vacuuming, brushing, wiping). A typical nuclear glovebox dismantling process involves cutting, drilling, and disassembling of contaminated objects, and can generate a consequent amount of hazardous debris [10]. Because of these operations, an accumulation of various objects, tools and debris can result in a cluttered environment causing operations disruptions, the accumulation of hazardous debris, and airborne contamination [10].

Three non-abrasive methods are available for the robotic manipulator arm to guarantee the glovebox surface cleanliness from debris [3]. Firstly, vacuum cleaning offers a fast and reliable way to collect large debris amounts on uncluttered surfaces. However, a vacuum cleaner can suck up unwanted or significant objects in a cluttered environment, resulting in tool clogging; and overall is a less controlled process which is undesirable in a Nuclear environment. Secondly, wet wiping techniques provide a high level of decontamination but are limited to residual quantities of debris collection on clean surfaces. Finally, brushing techniques for debris collection offer the advantage of removing large debris quantities using brush deflection properties, access to narrow gaps and safe interaction with surrounding objects. The particle removal mechanism involves two forces and one moment, the lifting and sliding forces, and the rolling moment [8]. The lifting force allows lifting debris particles from a surface; it must be larger than the adhesion force. The sliding force allows a particle to slide on a surface. The remove a particle, the sliding force must be superior to the difference between adhesion and lifting force multiplied by the coefficient of friction. The rolling moment allows the roll of debris particles on a surface; it depends on the debris particle shape and size. The rolling moment condition can be attained quickly for spherical and small debris. It is more challenging for cubic and large debris to reach the rolling moment debris removal conditions [8]. Also, the contact forces creating the condition of debris removal are located between the brush bristles, the debris and the surface. A theoretical contribution involved using a finite element model for brush debris interaction using a single bristle modelisation [1]. It analysed the influence of brush penetration using bristle deflection properties on debris removal forces and moments. The results indicate that the effective removal mechanisms are the horizontal sliding force and the rolling moment, the lifting force in a non-sticky environment. Also, the penetration has a beneficial impact when it is relatively small. Another practical contribution, limited to rotating brushes on road sweepers, indicates that debris removal depends on the interaction of several factors. These factors are the brush angle of attack,

the penetration, the rotational speed, coefficient of friction, bristle length, vehicle velocity and stick-slip friction cycles [20]. Powered brushing tools have been considered inappropriate for this environment, as to minimise the amount airborne contaminant and remove the need to develop the rad-hard tooling, compared to a cheap robust brush.

The long term goal is to make robot autonomously removing contaminated debris from nuclear gloveboxes. The robotic manipulator must be able to perform compliant and non-prehensile manipulation of a pile of debris from one position to another. This requires the manipulator to have the ability to set and control the brushing operative parameters. Several studies have focused on compliant robotic manipulator motion control with a linear brush tool for debris removal [9], [4], [17], [11], [15], [24]. These studies contributed by using conventional or data-driven control techniques and path planning approaches. However, they do not focus on task effectiveness and are not proven effective in our condition. Our operative condition imposes sweeping particles such as Beryllium, dust, sand, concrete, metallic swarf and bits of plastic. Thus, to control the robot and perform effective debris removal, the robot needs to set the correct operative brush parameters according to debris type and there are significant consequences of setting up the sub-optimal brushing parameters. For example, a high brush penetration increases brush wear and reduce sweeping effectiveness [12], [23]. Another challenge in sweeping processes is the "Backward sweeping" effect caused by debris sticking to the brush bristles. Pieces of debris stuck in the brush bristles are reapplied to surfaces at the next sweeping travel, decreasing the sweeping effectiveness and making the cleaning process ineffective [12], [23].

With the objective of an effective robotic sweeping process, it is important to understand the environmental and operative conditions affecting debris removal effectiveness. The effectiveness of operational brushing parameters for sweeping was explored in other field such as road cleaning [12], [23], [19], [20], surface polishing [16], solar panel cleaning [5] and duct cleaning [7]. Regarding their application, these studies involved rotating brushes, which are very effective for surface debris removal but not suitable for debris manipulation. Due to the high-velocity rotation, a rotating brush can also be unsafe for surfaces and surrounding objects, and risk creating airborne contaminants which undesirable. These studies also concluded that the effectiveness of a sweeping process depends on both environment and operational parameters [12], [23]. Environmental parameters refer to elements such as the surface roughness, the friction coefficient and the particle size of the debris to remove [23], [21], [20], [1]. Operational parameters refer to brush operational parameters, such as the brush angle of attack, brush penetration, the sweeping travel length and linear and rotational velocity. Moreover, there is limited research related to brushing application in the literature, and we could not find research studies related to debris removal application using linear brushes.

The paper builds on the research on robotic debris removal effectiveness by examining the operational brush condition and investigating their effect on debris removal. The sweeping test are performed using a 7 degrees-of-freedom robotic manipulator arm equipped with a brush. The surface to sweep is composed of polished stainless steel to match actual glovebox condition, and the tests are conducted using a 38 mm linear nylon brush with three debris sets. The tested debris particles set are flour, sand and metallic swarf. Also, we choose flour for simulating hazardous debris like Beryllium. The surface is considered smooth, and the debris particles are dry and easy to remove. Thus, we limit the experiment to two operative brush parameters, the brush angle of attack and penetration. The brush angle of attack is chosen to create a contact surface between the brush and debris, and the brush penetration is chosen to create a bond between the brush and surface. Because the surface is smooth, the friction between the debris and surface are considered low. Then, the other brush operative parameter are fixed, and the experiments have the same sweeping linear velocity (0.1m/s) and sweeping travel (150 mm) for all the tests. Also, this focuses the investigation on a slow and long sweeping sliding pattern allowing to limit airborne contamination. This study aims to ascertain whether the tested operational brush parameter affects debris removal effectiveness regarding the type of debris tested. In addition, the result of this study provides data paving the way towards the requirements for autonomous and robotic sweeping system.

In this paper, section 2 describes the materials and methods used during this experiment. Then in Section 2.1 details about the experimental setup are given, followed by the different types of debris components (section 2.2), the debris removal task (Section 2.3) and the experimental methodology (Section 2.4). Section 3 provides the result of the sweeping experiment for flour (Section 3.1), sand (section 3.2) and metallic swarf (Section 3.3). Then, Section 4 discusses the results of the debris removal experiment. Lastly, Section 5 presents the main conclusions resulting from this work.

2 Materials and Methods

2.1 Experimental Setup

Fig.1 represent the experimental setup components. The first component is the glovebox, where the experiment consists of sweeping a 150x100mm stainless steel flat and horizontal surface. The following components are the robotic manipulator arms (Kinova UltraLigth Gen 3) performing the sweeping task equipped with a 38mm nylon brush. The robot manipulator arm grasps the brush through a rigid mechanical interface (Fig.2a). Sweeping results pictures are captured with a Digital Single Lens Reflex Camera installed on a fixed tripod (Canon EOS 700D). The camera is installed on the top of the sweeping scene with constant and controlled lighting conditions (Fig.2b).

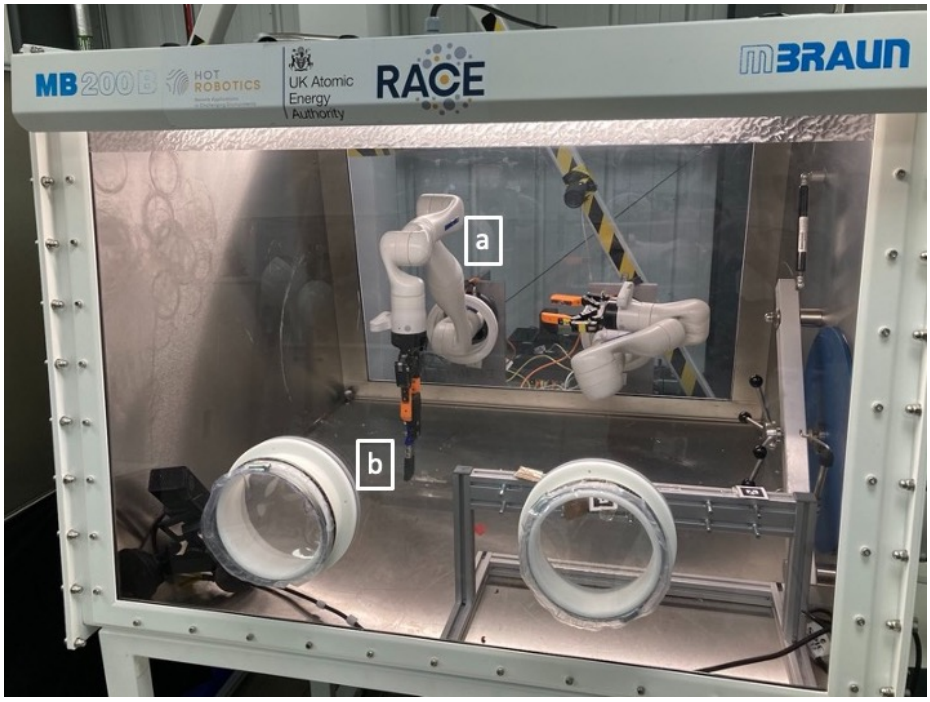

Fig. 1: Robot assisted nuclear glovebox composed of a pair of robotic manipulator (a) holding the brush tool (b)

(a) Robotic manipulator holding the brush in the end effector

(b) DSRL camera used to capture the images

Fig. 2: Robot Assisted Nuclear Glovebox Experimental Setup

2.2 Debris Components

For this research, the tested piles of debris are flour, sand and metallic swarf (Fig.3). In addition, for health and safety reasons, the piles of debris tested in this experiment are not the debris collected in actual operational conditions. Beryllium oxide, a toxic material, is replaced with wheat flour as they have both the same colour and particle size despite having different density (0.59 g/cm^3 for wheat flour vs 3.02 g/cm^3 for Beryllium) [22] [14]. The debris chosen offers various mechanical characteristics and properties regarding debris nature. Flour is a compressible and cohesive product where the friction angle decrease with pressure applied on the surface [6]. In addition, the typical particle size for commercial wheat flour is 20μm [6]. Unlike flour, sand is a non-compressible product and the friction angle increase with the pressure applied to the surface. Sand has a bigger particle size comprised between 20μm to 100μm [6]. The third debris type chosen is metallic swarf, and it is an abrasive and rigid type of debris. We have not assessed the average particle size for this type of debris. However, five samples were measured, showing a particle size comprised between 0.5mm to 70mm. For all debris types, we could not determine the precise friction coefficient. The tested debris were dry and the air relative humidity was 52% during the experiment.

Fig. 3: Debris Samples : flour, sand and metallic swarf (from left to right).

2.3 Debris removal task

The robotic manipulator arm performs the debris removal task, consisting of a repeated sweeping movement following a vertical rectangle shape (Fig.4). Also, the robot manipulator control software comprises a sweeping waypoint generator and a cartesian impedance controller (Fig.6). The sweeping waypoint generator generates the cartesian end-effector position and orientation, allowing a rectangle shape sweeping task to perform. It also offers five parameter settings: sweeping starting point, brush angle of attack, brush penetration, sweeping velocity, and sweeping travel length. All experiments were carried out using a fixed sweeping velocity of 0.1m/s and a sweeping travel length of 150 cm, they are chosen for providing a consistent and slow sweeping pattern. A slow and consistent sweeping pattern is needed to limit the energy transferred between the brush bristles and debris particles, thus limiting lifting force and potential airborne contamination. Also, the brush starting point, the brush angle of attack (Fig.5a) and the brush penetration (Fig.5b) are set and define before the experiment run. During the experiment, the brush angle of attack is set to 70, 80 and 90 degrees on the sweeping waypoint generator. As the brush angle of attack's modification is affecting the sweeping pattern and brush penetration, they were adjusted simultaneously to reach the desired starting point and brush penetration value. The brush penetration was set to 0,0.5 and 1 cm, and the verification was done using a centimetre graduated ruler. The sweeping starting point end-effector position was controlled using a 150x38mm frame stuck to the glovebox surface. The control system software performs ten sweeping movements for each experiment set before stopping. To conclude, the sweeping pattern movement is aimed to be consistent during all the sweeping travel with low velocity (0.1m/s). As the piles of debris are pushed, we do not use the dynamical brush property to expel debris from bristles.

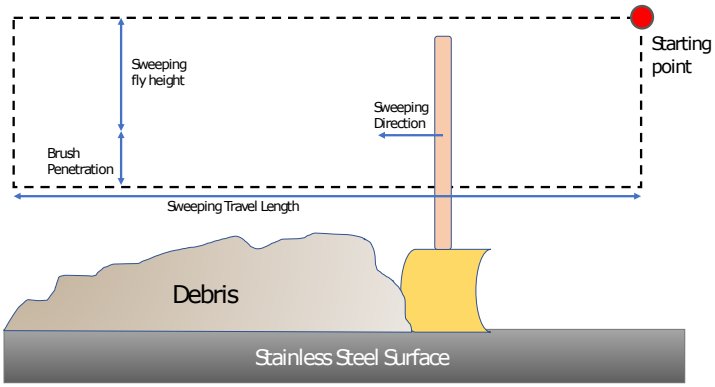

Fig. 4: Debris Removal Pattern

(a) Brush Angle of Attack (b) Brush Penetration

Fig. 5: Brush Operational Parameters

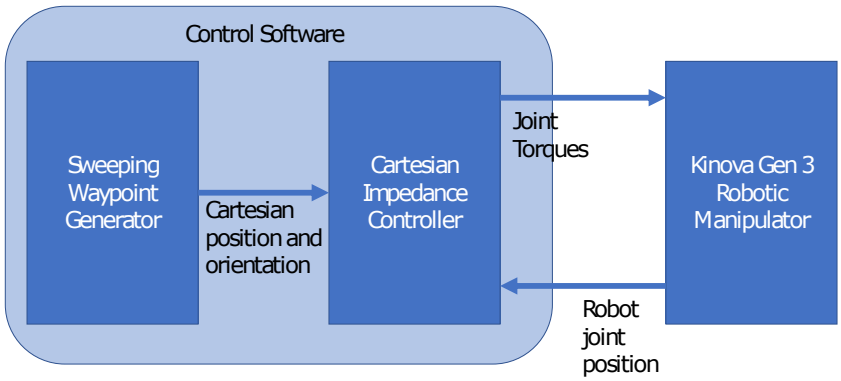

Fig. 6: Debris Removal Control Scheme

2.4 Testing Methodology

In this experiment, sweeping tests were carried out to evaluate whether brush angle of attack and brush penetration impacts the debris removal rate. Before performing the debris removal test, piles of debris are uniformly and consistently spread to cover all the sweeping test surfaces. The brush of angle attack and penetration was then set and verified using a ruler. Then, an experiment is carried out with the robot performing ten consecutive sweeping movements. After each sweep, a picture of the surface is taken and recorded on a computer. Each experiment is repeated five times to verify the sweeping debris removal rate consistency.

The sweeping effectiveness is evaluated using visual inspection with the help of a DSLR camera positioned at the height of 60 cm from the sweeping scene. Thereby, a picture is taken after each sweeping movement, as shown in Fig.7a. Then, for an experiment comprising ten sweeping movements, 11 pictures are

taken.

After the sweeping test, the debris removal effectiveness is calculated. Fig.7b illustrate the image process pipeline allowing to determine the Debris Removal Effectiveness (DRE). Each image is processed using a Matlab script performing the following action: crop the image to the cleaning frame, perform a greyscale transform (0-255), perform a brightness and contrast adjustment, count the pixel considered as part of debris and finally calculate the Debris Removal Effectiveness. For sand and metallic swarf, the brightness and contrast were adjusted to render the debris as dark pixels and the surface white. Pixels under a 70 greyscale level were considered debris. In the flour case, the brightness and contrast were adjusted to render the flour particle white and the surface darker, and pixel-level above a 200 greyscale level was considered debris. The Matlab script calculates the Debris Removal Effectiveness (DRE, Eq.1) by calculating the ratio of clean area pixels over the total number of pixels for each picture on an experimental set.

$$DRE = (\frac{TP - DP}{TP}) * 100 \tag{1}$$

Where TP represent the total number of pixels in the cropped image and DP represents the total number of pixels where debris is present.

Hence all Debris Removal Effectiveness are calculated for all pictures in an experimental set; we want to verify result consistency. Then, we calculate the mean (Eq.2) and standard deviation (Eq.3) for each iteration sweep regarding the five experimental repetition sets such:

$$MDRE_i = \frac{1}{n} \sum_{j=1}^{n} DRE_j \tag{2}$$

$$\sigma_i = \sqrt{\frac{1}{n-1} \sum_{j=1}^{n} (DRE_j - MDRE_i)^2} \tag{3}$$

With n corresponding to the number of sweeping tests performed, five times in our case, and i correspond to the sweeping index in a sequence of consecutive sweeping.

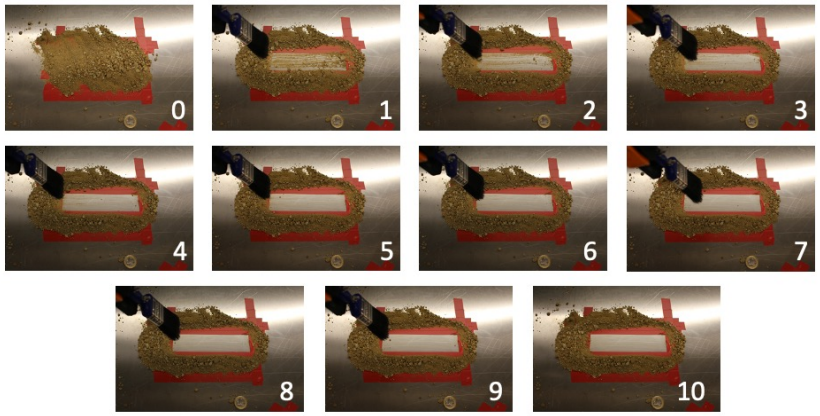

(a) Debris Removal Operation Process

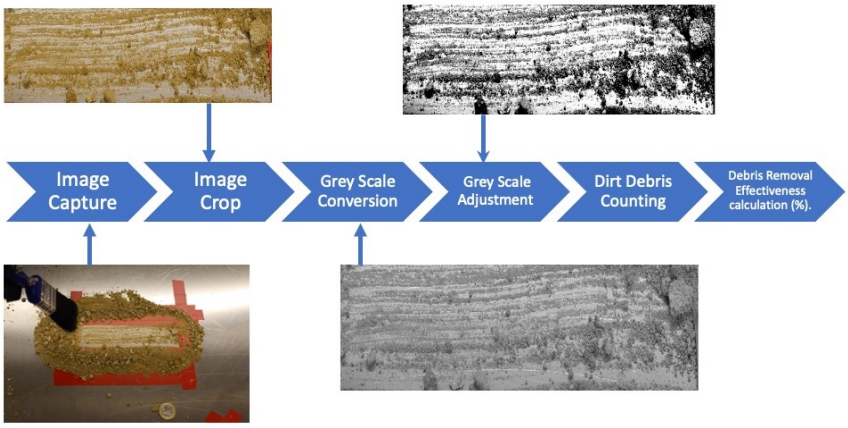

(b) Data Processing Pipeline

Fig. 7: Debris Removal Operation Process and Data Processing

3 Result and Analysis

3.1 Flour debris removal

Fig.8a. presents the mean debris removal effectiveness regarding the number of consecutive sweepings for an angle of attack of 70 degrees and with a penetration of 0 cm, 0.5 cm and 1 cm. Despite having different brush penetration, the mean debris removal effectiveness results are very close and fluctuate around an average value of 99.6%. The mean debris removal effectiveness fluctuation results from backward sweeping, which also increases the variability of results in any case. As a large brush surface is in contact with the debris, the debris particles tend to get caught in the brush bristles and are reapplied to the surface. On this angle of attack configuration, the first sweep catches a large debris amount that is then evacuated from the bristles thanks to the considerable brush bristle deflection on each consecutive sweep. After ten consecutive sweeps, the mean debris removal effectiveness attains 99.86 % with 1 cm penetration, 99.61% with 0.5 cm penetration, and 99.62% with 0 cm brush penetration.

Fig.8b presents results for a brush angle of attack of 80 degrees with 0 cm, 0.5 cm and 1 cm penetration. A backward sweeping of flour particles appears in any configuration and degrades the initial sweeping effectiveness despite a very high first sweep. Also, in each configuration and after the first sweep, the Debris Removal Effectiveness decreases until the sixth sweep. Thereafter, it increases as the brush deflection evacuates the debris from the bristles. The standard deviation for the three configurations overlaps, and it is difficult to determine the best configuration. However, the configuration with 0.5 cm brush penetration has the least standard deviation. After ten consecutive sweeps, the mean debris removal effectiveness attains 99.84 % with 1 cm penetration, 99.90% with 0.5 cm penetration, and 99.88% with 0 cm brush penetration.

Fig.8c presents results for a brush angle of attack of 90 degrees with 0 cm, 0.5 cm and 1 cm penetration. The best brush penetration results are the 0.5 cm and 1 cm configurations. A performance of 0 cm gives the lower performance as this configuration offers the lower contact between the brush, the surface and debris. The backward sweeping effect is less important with a brush angle of attack of 90 degrees, thanks to the reduced surface of contact between the brush and the debris. After ten consecutive sweeps, the mean debris removal effectiveness attains 99.85% with 1 cm penetration, 99.86% with 0.5 cm penetration, and 97.12% with 0 cm brush penetration.

3.2 Sand debris removal

Fig.9a presents results for a brush angle of attack of 70 degrees with 0 cm, 0.5 cm and 1 cm penetration. In any configuration, the sweeping effectiveness after the first sweep starts low (around 67% removal effectiveness) as the friction between the debris and the surface makes the removal challenging. At least three

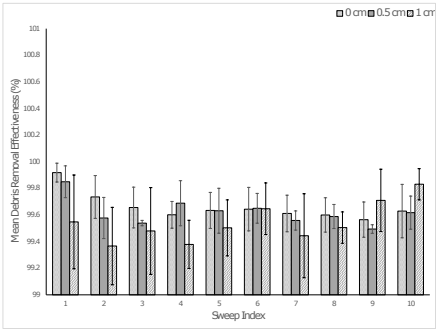

(a) Angle of Attack: 70 degrees

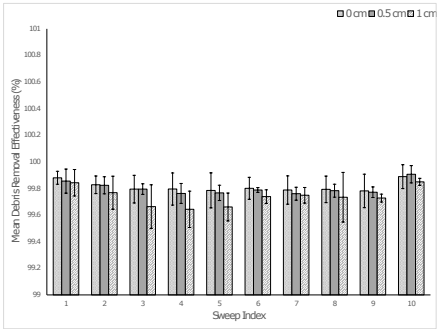

(b) Angle of Attack: 80 degrees

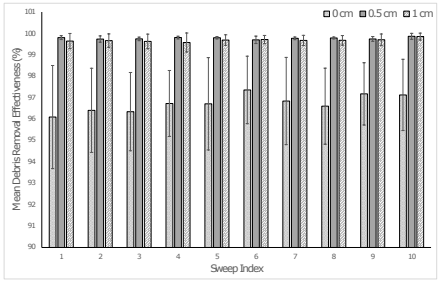

(c) Angle of Attack: 90 degrees

Fig. 8: Mean Debris Removal Effectiveness for Flour debris

sweeps are necessary to attain a removal rate of 90%, and after ten sweeps, the effectiveness is more than 95% in any case. The fluctuation of performance between the fourth and eighth sweeping is caused by the backward sweeping effect reapplying debris on the surface to clean as an angle of 70 degrees induces a high surface of contact with the brush. After ten consecutive sweeps, the mean debris removal effectiveness attains 99.58% with 1 cm penetration, 98.83% with 0.5 cm penetration, and 97.07% with 0 cm brush penetration.

Fig.9b presents results for a brush angle of attack of 80 degrees with 0 cm, 0.5 cm and 1 cm penetration. As it seems that the friction coefficient is high between the building sand and the surface, the least effective configuration is given by a brush penetration of 0 cm. A better mean debris removal effectiveness is provided by brush penetration of 0.5 cm and 1 cm. However, the overlap of standard deviation does not provide enough information to determine which configuration offers the best outcome. After ten consecutive sweeps, the mean debris removal effectiveness attains 98.65% with 1 cm penetration, 96.94% with 0.5 cm penetration, and 91.46% with 0 cm brush penetration.

Fig.9c presents results for a brush angle of attack of 90 degrees with 0 cm, 0.5 cm and 1 cm penetration. In this angle of attack configuration, the best perfor-

mance is given by a brush penetration of 0.5 cm. After ten consecutive sweeps, the mean debris removal effectiveness attains 96.76% with 1 cm penetration, 97.14% with 0.5 cm penetration, and 95.17% with 0 cm brush penetration.

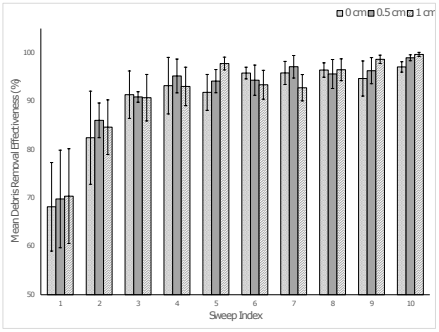

(a) Angle of Attack: 70 degrees

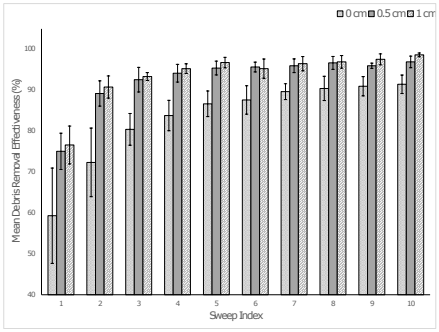

(b) Angle of Attack: 80 degrees

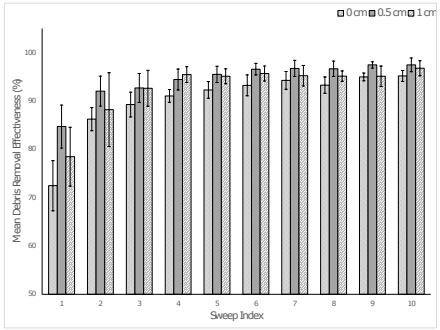

(c) Angle of Attack: 90 degrees

Fig. 9: Mean Debris Removal Effectiveness for Sand debris

3.3 Metallic Swarf debris removal

Fig.10a presents results for a brush angle of attack of 70 degrees with 0 cm, 0.5 cm and 1 cm penetration. After three sweeps, all penetration configurations make the sweeping removal effectiveness rate fluctuate between 94% and 100% without sign of stabilisation and with a large standard and overlapping standard deviation. This phenomenon is due to backward sweeping, where the metallic swarf particles are firmly caught in brush bristles. The backward sweeping effect is stronger with 1 cm and 0.5 cm brush penetration. After ten consecutive sweeps, the mean debris removal effectiveness attains 99.39% with 1 cm penetration, 99.85% with 0.5 cm penetration, and 99.89% with 0 cm brush penetration. At the end of the testing procedure and for all operational brush configurations,

the brush has metallic swarf blocked into the brush bristles.

Fig.10b presents results for a brush angle of attack of 80 degrees with 0 cm, 0.5 cm and 1 cm penetration. From the first sweep, all penetration configurations make the sweeping removal effectiveness rate fluctuate between 95% and 99% without sign of stabilisation and with a large standard and overlapping standard deviation. The backward sweeping effect is stronger with 1 cm, and 0.5 cm brush penetration as the metallic swarf particles are caught within the brush bristles. After ten consecutive sweeps, the mean debris removal effectiveness attains 98.79% with 1 cm penetration, 98.30% with 0.5 cm penetration, and 98.74% with 0 cm brush penetration. At the end of the testing procedure and for all operational brush configurations, the brush has metallic swarf blocked into the brush bristles.

Fig.10c presents results for a brush angle of attack of 90 degrees with 0 cm, 0.5 cm and 1 cm penetration. After ten consecutive sweeps, the mean debris removal effectiveness attains 98.74% with 1 cm penetration, 98.84% with 0.5 cm penetration, and 95.09% with 0 cm brush penetration. In any configuration, the limitation of surface contact between the brush and debris limits the backward sweeping effect. However, this also affects the sweeping mean debris removal effectiveness, depending on the brush penetration. A higher penetration indicates a better contact between the brush and surface that seal potential debris leak. At the end of the testing procedure and for all operational brush configurations, the brush has metallic swarf blocked into the brush bristles. The 90 degrees brush angle of attack configuration offers a more consistent result than the 70 degrees and 80 degrees brush angle of attack.

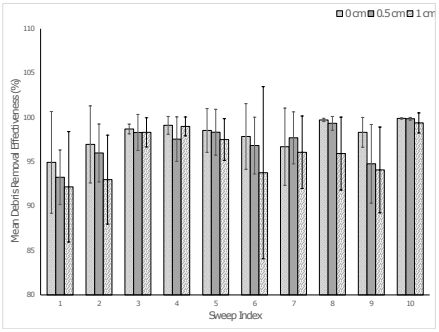

(a) Angle of Attack: 70 degrees

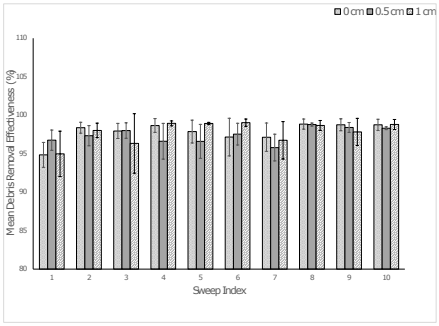

(b) Angle of Attack: 80 degrees

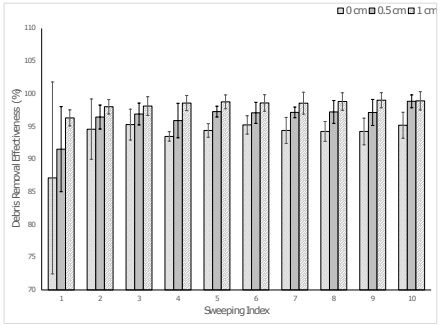

(c) Angle of Attack: 90 degrees

Fig. 10: Mean Debris Removal Effectiveness for Metallic Swarf debris

4 Discussion

For any debris type, we observe an influence of the brush parameter on the debris removal effectiveness. Depending on the debris type and the brush configuration parameter, debris removal effectiveness varies significantly with a greater influence from the brush angle of attack. In the case of flour, removing large quantities of debris from a stainless-steel surface is easy as there is low friction between the debris and surface. For example, an 80 degrees angle of attack and a 0.5 cm brush penetration offer 99.90% mean debris removal effectiveness after ten consecutive sweeps, which can be considered the best configuration for this debris type. On the contrary, the lowest performance has been attained with a brush penetration of 0 cm combined with a brush angle of attack of 90 degrees. Despite removing a 97.12% of debris after ten sweeps, this configuration is the least effective because it does not create sufficient contact for debris removal. The brush misses debris particles on the surface to clean. For configuration offering an angle of attack of 70 degrees or 80 degrees, we can observe the sweeping mean debris removal effectiveness degradation after the first sweep. These degraded performances are due to backward sweeping resulting from high surface contact between the brush bristle and the small flour particle size. After the first sweep, flour debris parti-

cles are stuck within the brush bristle. Then, on the following sweep and during brush deflection, the debris particles are released on the surface, causing degradation of debris removal performance.

For sand debris, it appears that the removal of debris is more challenging compared to flour. Friction increases when an increasing compression force is applied to the product. For all configurations, the sweeping effectiveness starts lower than other debris types. For example, after the first sweep, the average mean debris removal effectiveness is 73.34% for sand for all operational configurations. Thereby, 70 degrees brush angle of attack offers the best debris removal effectiveness. However, the mean debris removal standard deviation overlaps and does not allow us to evaluate the impact of brush penetration on debris removal effectiveness.

Metallic swarf is the most challenging debris type despite being easy to remove. As metallic swarf has a thread shape combined with abrasiveness and rigid properties, this type of debris particles can quickly get stuck into the brush bristles, resulting in backward sweeping. Unlike debris like flour or sand, the operational condition that offers the best debris removal effectiveness result is given by a brush angle of attack of 90 degrees and a brush penetration of 1 cm resulting in 99.89%. Indeed, to limit the backward sweeping effect, it is important to limit the debris-bristles contact surface. In all configurations, the debris removal effectiveness is degraded because of backward sweeping.

Moreover, backward sweeping is a recurring issue met with any debris. Certain operational conditions must be avoided to limit the impact of this effect. This challenge must be considered in actual conditions as it could degrade cleaning effectiveness. Therefore, to avoid backward sweeping, the robot must limit the brush-debris contact surface and must be maximised for compressible product such as flour, balanced for non compressible product like sand and minimised for swarf shape debris. For an autonomous robot, other possible ways to resolve the backward sweeping problem would be to perform movement patterns with small travel lengths and use the brush mechanical properties dynamics which were not assessed in this study.This way, the brush is deflected to load energy and release the energy resulting in debris expel and less debris stuck in the bristles. The sweeping robot movement limiting backwards sweeping is in contradiction with the airborne limitation requirement. Then, the robot must autonomously find the balance between limiting backwards sweeping and airborne contamination.

The result shows that in all configurations and after ten sweeps, the debris removal effectiveness attains more than 90% for any type of debris. This indicates that repeating the same sweeping movement multiple times improves the cleanliness of a surface for high friction products. For flour, 95% debris removal effectiveness can be attained after one sweep, where four sweeps are needed in the sand case. For metallic swarf, the debris removal dynamics attain 95% after

the third sweep but have more variability because of swarf caught in brush bristles, and multiple sweeps can decrease the debris removal effectiveness. Within the same condition, the variation of debris removal effectiveness dynamics could be caused by the debris friction, size and the compressibility property. In regards to autonomous robot control, an effective control must adapt the number of sweeps to reach a given clean surface requirement. This adaptive robot control is important to avoid brush wear, surface attrition and backward sweeping.

Finally, for an autonomous and adaptive robotic manipulator arm to be effective in debris removal operation, the robot must identify the debris parameter (friction coefficient, particle size, compressibility property), the brush parameter (bristle length and stiffness) and the surface roughness. Knowing these parameters would allow the robot to adapt to the environment and situation and determine the required task and path planning.

5 Conclusion

This paper shows an effective method for developing a robotic sweeping system and selecting the correct brushing parameters. Debris removal effectiveness has been tested on flour, sand and metallic swarf on a stainless steel using a robotic manipulator. Regarding the operational brush conditions, the tested brush angle of attacks were 90 degrees, 80 degrees and 70 degrees, and the tested penetrations were 0 cm, 0.5 cm and 1 cm. The test was performed using a 7 DOF robot manipulator handling a 38mm nylon brush repeating a rectangle shape sweeping pattern with a cartesian impedance controller. Sweeping debris removal effectiveness was evaluated using visual inspection methods.

The results show that the operational brush parameter must be adjusted following the type of debris to remove from the surface. Firstly, for ultra-fine particles such as flour, the best removal effectiveness is given by a moderate angle of attack (80 degrees) and a moderate penetration (0.5 cm). This configuration pressures the debris and limits the backward sweeping effect. Secondly, the best removal effectiveness for fine particles like sand is given by the lowest angle of attack (70 degrees) independently of the brush penetration. As sand seems to have the highest friction coefficient of the tested debris, more pressure is needed to remove the debris particle. Finally, despite being easy to remove, metallic swarf debris necessitates a high angle of attack (90 degrees) with high penetration (1 cm). This type of debris necessitates a little surface of contact between the brush and debris combined with a high pressure between the brush and the surface.

This preliminary study identifies the performance and issues met during the robotic sweeping process for debris removals in the limit of the debris and operational parameter tested. However, a broader spectrum of particle size distribution

and operational brush parameters must be tested in the future. About the particle size distribution, a mix of different types of debris, including a large particle size distribution and a mix of particle size friction, would be essential to observe and analyse the sweeping performance. Regarding the development of robotic and autonomous sweeping system for nuclear glovebox, future work must focus on the debris parameter identification (particle size, friction), task planning adapting to debris type and path planning adapting to glovebox environment.

6 Acknowledgements

This project has been supported by the RAIN Hub, which is funded by the Industrial Strategy Challenge Fund, part of the government's modern Industrial Strategy. The fund is delivered by UK Research and Innovation and managed by EPSRC [EP/R026084/1].

References

1. Abdel Wahab, M.M., Wang, C., Vanegas Useche, L.V., Parker, G.: Finite element models for brush-debris interaction in road sweeping. Acta Mechanica **215**(1-4), 71–84 (2010). https://doi.org/10.1007/s00707-010-0304-y
2. Bayliss, C.R., Langley, K.F.: Chapter 11 - Dismantling Techniques. pp. 99–111. Nuclear Decommissioning, Waste Management, and Environmental Site Remediation, Butterworth-Heinemann, Burlington (2003). https://doi.org/https://doi.org/10.1016/B978-075067744-8/50014-X, https://www.sciencedirect.com/science/article/pii/B978075067744850014X
3. Bayliss, C., Langley, K.: Decontamination Techniques. In: Bayliss, C.R., Langley, K.F. (eds.) Nuclear Decommissioning, Waste Management, and Environmental Site Remediation, pp. 89–97. Nuclear Decommissioning, Waste Management, and Environmental Site Remediation, Butterworth-Heinemann, Burlington (2003). https://doi.org/10.1016/b978-075067744-8/50013-8, https://www.sciencedirect.com/science/article/pii/B9780750677448500138
4. Bormann, R., Hampp, J., Hagele, M.: New brooms sweep clean - An autonomous robotic cleaning assistant for professional office cleaning. Proceedings - IEEE International Conference on Robotics and Automation **2015-June**(June), 4470–4477 (2015). https://doi.org/10.1109/ICRA.2015.7139818
5. Chen, E.Y.T., Ma, L., Yue, Y., Guo, B., Liang, H.: Measurement of dust sweeping force for cleaning solar panels. Solar Energy Materials and Solar Cells **179**(August 2017), 247–253 (2018). https://doi.org/10.1016/j.solmat.2017.12.009, https://doi.org/10.1016/j.solmat.2017.12.009
6. Duroudier, J.P.: Mechanical Characteristics of Divided Solids. Divided Solids Mechanics pp. 1–56 (2016). https://doi.org/10.1016/b978-1-78548-187-1.50001-3
7. Holopainen, R., Salonen, E.M.: Modelling the cleaning performance of rotating brush in duct cleaning. Energy and Buildings **34**(8), 845–852 (2002). https://doi.org/10.1016/S0378-7788(02)00101-9
8. Kanegsberg, B.: Handbook for Critical cleaning, vol. 105 (2001). https://doi.org/10.1016/s0026-0576(07)80159-0
9. Leidner, D.S.: Cognitive Reasoning for Compliant Robot Manipulation. Doctoral Thesis p. 211 (2019), http://www.springer.com/series/5208

10. Office for Nuclear Regulation: NS-INSP-GD-053 - Criticality Safety pp. 1–29 (2020)
11. Okada, K., Kojima, M., Sagawa, Y., Ichino, T., Sato, K., Inaba, M.: Vision based behavior verification system of humanoid robot for daily environment tasks. Proceedings of the 2006 6th IEEE-RAS International Conference on Humanoid Robots, HUMANOIDS pp. 7–12 (2006). https://doi.org/10.1109/ICHR.2006.321356
12. Peel, G., Michielen, M., Parker, G.: Some aspects of road sweeping vehicle automation. IEEE/ASME International Conference on Advanced Intelligent Mechatronics, AIM **1**, 337–342 (2001). https://doi.org/10.1109/aim.2001.936477
13. Regulation, N.: Investigation into the Thermal Oxide Reprocessing Plant (THORP) contamination event (August 2016), 1–15 (2017)
14. Snead, L.L., Zinkle, S.J.: Use of beryllium and beryllium oxide in space reactors. AIP Conference Proceedings **746**(March 2005), 768–775 (2005). https://doi.org/10.1063/1.1867196
15. Sri Vishva, R., Naresh, R., Venkada Krishnan, M.S.: An Autonomous Cleaning Robot. Proceedings - International Conference on Artificial Intelligence and Smart Systems, ICAIS 2021 pp. 686–691 (2021). https://doi.org/10.1109/ICAIS50930.2021.9395909
16. Stango, R.J., Cariapa, V., Prasad, A., Liang, S.K.: Measurement and analysis of brushing tool performance characteristics, part 1: Stiffness response. Journal of Manufacturing Science and Engineering, Transactions of the ASME **113**(3), 283–289 (1991). https://doi.org/10.1115/1.2899698
17. Sun, G., Li, P., Yu, Z., Chen, Z., Zhou, Y., Yue, L., Liu, Y.H.: Task-oriented impedance control for integrated autonomous cleaning manipulator. IEEE International Conference on Robotics and Biomimetics, ROBIO 2019 (December), 358–363 (2019). https://doi.org/10.1109/ROBIO49542.2019.8961483
18. Tokatli, O., Das, P., Nath, R., Pangione, L., Altobelli, A., Burroughes, G., Jonasson, E.T., Turner, M.F., Skilton, R.: Robot-assisted glovebox teleoperation for nuclear industry. Robotics **10**(3) (2021). https://doi.org/10.3390/robotics10030085
19. Vanegas-Useche, L.V., Abdel-Wahab, M.M., Parker, G.A.: Determination of friction coefficients, brush contact arcs and brush penetrations for gutter brush-road interaction through FEM. Acta Mechanica **221**(1-2), 119–132 (2011). https://doi.org/10.1007/s00707-011-0490-2
20. Vanegas-Useche, L.V., Abdel-Wahab, M.M., Parker, G.A.: Effectiveness of oscillatory gutter brushes in removing street sweeping waste. Waste Management **43**, 28–36 (2015). https://doi.org/10.1016/j.wasman.2015.05.014, http://dx.doi.org/10.1016/j.wasman.2015.05.014
21. Vanegas Useche, L.V., Wahab, M.M., Parker, G.A.: Effectiveness of gutter brushes in removing street sweeping waste. Waste Management **30**(2), 174–184 (2010). https://doi.org/10.1016/j.wasman.2009.09.036, http://dx.doi.org/10.1016/j.wasman.2009.09.036
22. Virji, M.A., Stefaniak, A.B., Day, G.A., Stanton, M.L., Kent, M.S., Kreiss, K., Schuler, C.R.: Characteristics of beryllium exposure to small particles at a beryllium production facility. Annals of Occupational Hygiene **55**(1), 70–85 (2011). https://doi.org/10.1093/annhyg/meq055
23. Wang, C.: Brush M odelling and Control Techniques for Automatic Debris Rem ova l during Road Sweeping. Ph.D. thesis, University Of Surrey (2005)
24. Ye, G., Alterovitz, R.: Guided Motion Planning. Robotics Research pp. 291–307 (2017)